

## Assembling Hierarchical Cluster Solids with Atomic Precision

Ari Turkiewicz,<sup>†</sup> Daniel W. Paley,<sup>†</sup> Tiglet Besara,<sup>‡</sup> Giselle Elbaz,<sup>†</sup> Andrew Pinkard,<sup>†</sup> Theo Siegrist,<sup>‡,§</sup> and Xavier Roy<sup>\*,†</sup>

<sup>†</sup>Department of Chemistry, Columbia University, New York, New York 10027, United States

<sup>‡</sup>National High Magnetic Field Laboratory, Florida State University, Tallahassee, Florida 32310, United States

<sup>§</sup>Department of Chemical and Biomedical Engineering, FAMU-FSU College of Engineering, Tallahassee, Florida 32310, United States

### S Supporting Information

**ABSTRACT:** Hierarchical solids created from the binary assembly of cobalt chalcogenide and iron oxide molecular clusters are reported. Six different molecular clusters based on the octahedral  $\text{Co}_6\text{E}_8$  (E = Se or Te) and the expanded cubane  $\text{Fe}_8\text{O}_4$  units are used as superatomic building blocks to construct these crystals. The formation of the solid is driven by the transfer of charge between complementary electron-donating and electron-accepting clusters in solution that crystallize as binary ionic compounds. The hierarchical structures are investigated by single-crystal X-ray diffraction, providing atomic and superatomic resolution. We report two different superstructures: a superatomic relative of the CsCl lattice type and an unusual packing arrangement based on the double-hexagonal close-packed lattice. Within these superstructures, we demonstrate various compositions and orientations of the clusters.

We describe a family of binary solid-state compounds in which the fundamental building blocks are independently prepared, electronically and structurally complementary inorganic molecular clusters. Charge transfer between cobalt chalcogenide and iron oxide clusters generates atomically defined hierarchical assemblies<sup>1</sup> in which the intercluster electrostatic attractions form the binary superlattice. We demonstrate various levels of control over the structure of the material: (i) we modify the composition of the clusters while retaining the same cluster arrangement; (ii) we change the orientation of the cluster building blocks while retaining the same cluster superstructure; and (iii) we force the superstructure to adopt a different configuration that has polar symmetry.

Non-molecular compounds with identifiable cluster subunits (e.g., Chevrel and Zintl phases) can display remarkable materials properties,<sup>2–5</sup> but their solid-state syntheses from elemental or polyatomic precursors inhibit the rational tuning of their structure and properties. Assembling solid-state materials from preformed and intact nanoscale building blocks with well-controlled and tunable properties offers significant benefits over traditional solid-state reactions and is expected to lead to the realization of materials by design.<sup>6</sup> Each type of building block, however, comes with its own set of benefits and limitations. For instance, nanocrystals have been assembled into

remarkable superlattices, but these materials intrinsically lack atomic precision.<sup>7,8</sup> Molecular clusters with discrete, atomically defined structures can exhibit superatom-like collective properties<sup>9–11</sup> and offer rich chemistry.<sup>12</sup> Single-cluster-component functional materials<sup>12–17</sup> as well as binary cluster assemblies from charged precursors<sup>18,19</sup> or interconnected supertetrahedral clusters<sup>20</sup> have been prepared, but a generally applicable route toward crystallographically precise solids combining two or more cluster units remains an open issue.<sup>21,22</sup>

Our strategy for creating hierarchical binary assemblies of clusters was to use charge transfer between neutral clusters and subsequent intercluster electrostatic attraction as a driving force for co-assembly and crystallization. We designed, synthesized, and combined pairs of complementary molecular clusters in which one cluster is electron-donating and the other is electron-accepting.<sup>23–25</sup> Each building block is comprised of a redox-active core encapsulated in a protective redox-inert shell of ligands. These superatoms are shown in Figure 1 with their respective energy levels as measured by cyclic voltammetry (CV) (see Figures S32–S37). The octahedral clusters  $\text{Co}_6\text{Se}_8(\text{PET}_3)_6$ ,  $\text{Co}_6\text{Te}_8(\text{PET}_3)_6$ ,  $\text{Co}_6\text{Te}_8(\text{P}^n\text{Pr}_3)_6$ , and  $\text{Co}_6\text{Te}_8(\text{PET}_2\text{Ph})_6$  are electron-rich and can reversibly donate up to five electrons (the first four are shown in Figure 1). Conversely, the cubane clusters  $\text{Fe}_8\text{O}_4\text{pz}_{12}\text{Cl}_4$  and  $\text{Fe}_8\text{O}_4\text{pz}_{12}\text{Br}_4$  (pz = pyrazolide) are good electron acceptors and can reversibly take up to four electrons. Being electrically neutral, these donor and acceptor clusters are soluble in non-polar solvents such as toluene and benzene.

The respective redox potentials of  $\text{Co}_6\text{Te}_8(\text{PET}_3)_6$  and  $\text{Fe}_8\text{O}_4\text{pz}_{12}\text{Cl}_4$  indicate that the clusters undergo one-electron transfer in solution, though we recognize that the binary ionic lattice formation and symmetry will be further governed by the crystal lattice energy. We combined the clusters  $\text{Co}_6\text{Te}_8(\text{PET}_3)_6$  and  $\text{Fe}_8\text{O}_4\text{pz}_{12}\text{Cl}_4$  in toluene and after ~12 h obtained millimeter-sized black crystals that are insoluble in non-polar solvents but are very soluble in polar organic solvents such as dichloromethane and tetrahydrofuran. The solubility of these crystals is consistent with the formation of an ionic compound.

Single-crystal X-ray diffraction (SCXRD) established that the resulting solid is a 1:1 binary combination of the clusters (Figure 2), and powder X-ray diffraction confirmed the homogeneity of the crystalline phase. The internal structures

Received: August 30, 2014

Published: October 20, 2014

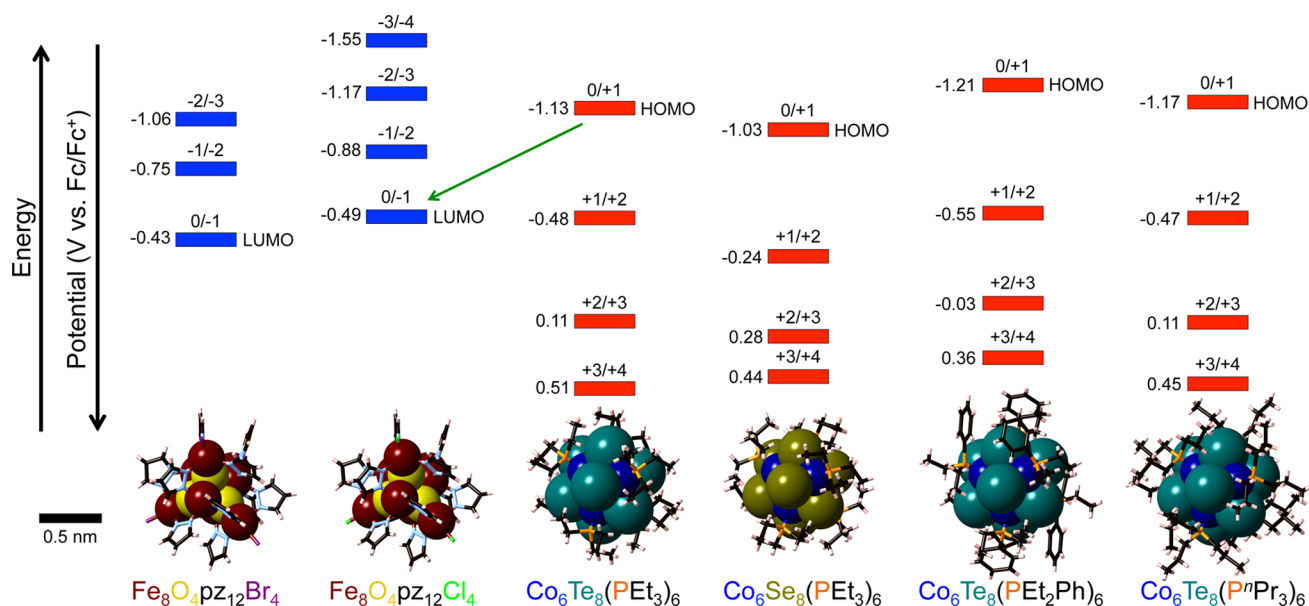


**Figure 1.** Molecular structures and redox potentials of the cluster building blocks as determined by SCXRD and CV. The clusters are depicted on the same size scale.

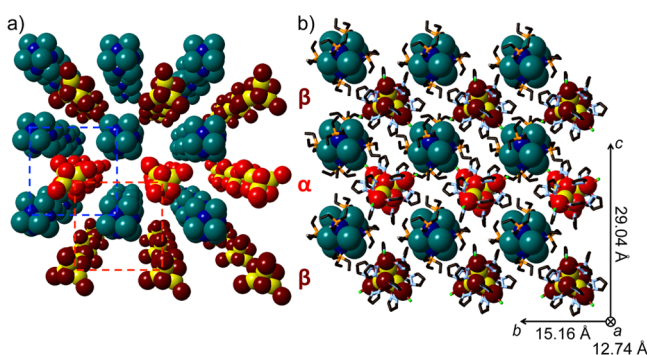


**Figure 2.** Crystal structure of  $[\text{Co}_6\text{Te}_8(\text{PEt}_3)_6][\text{Fe}_8\text{O}_4\text{pz}_{12}\text{Cl}_4]$  showing the crystal packing looking down the  $a$ -axis. (a) Perspective view with the capping ligands removed. (b) View displaying the position of the ligands. Fe, dark and light red; O, yellow; Co, dark blue; Te, teal; P, orange; N, light blue; Cl, green; C, black. Hydrogen atoms were omitted to clarify the views.

of the constituent clusters remain unchanged in the solid-state compound, and the overall packing of  $[\text{Co}_6\text{Te}_8(\text{PEt}_3)_6]$ -

$[\text{Fe}_8\text{O}_4\text{pz}_{12}\text{Cl}_4]$  can be approximated to a primitive cubic lattice with a two-cluster basis that is the superatomic analogue of the CsCl lattice type.<sup>26</sup> The atomic resolution of SCXRD allows us to discern subtle crystallographic variations in the orientation of the superatoms that lower the symmetry of the crystal. While  $\text{Co}_6\text{Te}_8(\text{PEt}_3)_6$  adopts a single orientation, the triclinic unit cell contains two  $\text{Fe}_8\text{O}_4\text{pz}_{12}\text{Cl}_4$  units related by an inversion center (clusters  $\alpha$  and  $\beta$  shown in bright red and dark red in Figure 2). Thus, layers of  $\text{Fe}_8\text{O}_4\text{pz}_{12}\text{Cl}_4$  are alternating along the  $c$ -axis between two inversion-center-related orientations. The centroid-to-centroid distance between two complementary adjacent clusters ranges from 11.81 to 12.75  $\text{\AA}$ .

Simple cubic superlattices are also obtained when we combine donor and acceptor clusters with sizes, core structures, and redox properties similar to those of  $\text{Co}_6\text{Te}_8(\text{PEt}_3)_6$  and  $\text{Fe}_8\text{O}_4\text{pz}_{12}\text{Cl}_4$ . The structures of the solid-state compounds  $[\text{Co}_6\text{Se}_8(\text{PEt}_3)_6][\text{Fe}_8\text{O}_4\text{pz}_{12}\text{Cl}_4]$ ,  $[\text{Co}_6\text{Te}_8(\text{PEt}_2\text{Ph})_6][\text{Fe}_8\text{O}_4\text{pz}_{12}\text{Cl}_4]$ , and  $[\text{Co}_6\text{Te}_8(\text{PEt}_3)_6][\text{Fe}_8\text{O}_4\text{pz}_{12}\text{Br}_4]$  all approximate the CsCl packing, but the crystallographic details of each solid differ. While the compounds  $[\text{Co}_6\text{Se}_8(\text{PEt}_3)_6][\text{Fe}_8\text{O}_4\text{pz}_{12}\text{Cl}_4]$  and  $[\text{Co}_6\text{Te}_8(\text{PEt}_3)_6][\text{Fe}_8\text{O}_4\text{pz}_{12}\text{Br}_4]$  adopt the

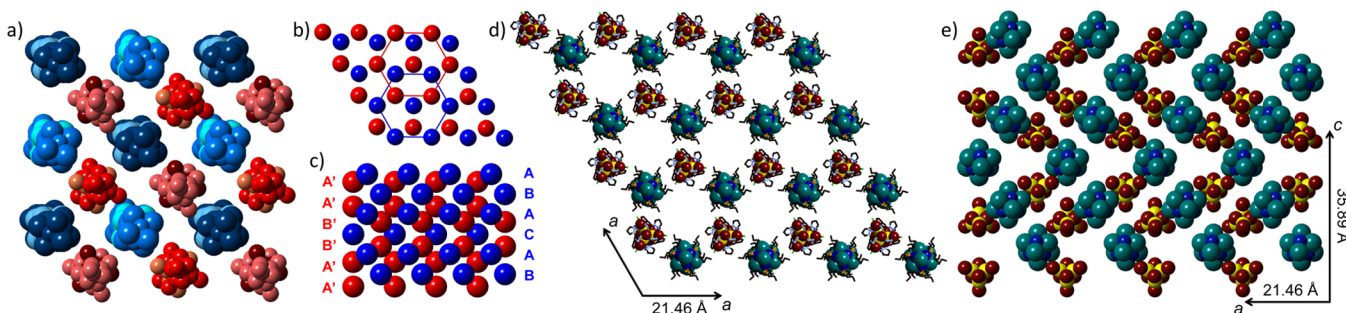


**Figure 3.** (a) Crystal structure of  $[\text{Co}_6\text{Te}_8(\text{PEt}_2\text{Ph})_6][\text{Fe}_8\text{O}_4\text{pz}_{12}\text{Cl}_4]$  showing the various orientations of the superatomic cation and anion as different shades of blue and red, respectively. (b,c) Schematic views of the crystal packing of  $[\text{Co}_6\text{Te}_8(\text{P}^n\text{Pr}_3)_6][\text{Fe}_8\text{O}_4\text{pz}_{12}\text{Cl}_4]$ . Cations are blue, and anions are red. (d,e) Crystal structure of  $[\text{Co}_6\text{Te}_8(\text{P}^n\text{Pr}_3)_6][\text{Fe}_8\text{O}_4\text{pz}_{12}\text{Cl}_4]$ . Panels (b) and (d) show views of a single hexagonal bilayer looking down the  $c$ -axis; panels (c) and (e) show the stacking sequence of the hexagonal layers along the  $c$ -axis. Capping ligands were removed in (a) and (e) to clarify the views. Colors as previously defined. Hydrogen atoms were omitted to clarify the views.

same triclinic unit cell as  $[\text{Co}_6\text{Te}_8(\text{PET}_3)_6][\text{Fe}_8\text{O}_4\text{pz}_{12}\text{Cl}_4]$  with slightly different lattice parameters (Table S1), the structure of  $[\text{Co}_6\text{Te}_8(\text{PET}_2\text{Ph})_6][\text{Fe}_8\text{O}_4\text{pz}_{12}\text{Cl}_4]$  is more complex. The substitution of a rigid phenyl group on the phosphine capping ligands forces each building unit to adopt four different orientations in the monoclinic unit cell (Figure 3a).

The cluster  $\text{Co}_6\text{Te}_8(\text{P}^n\text{Pr}_3)_6$  has the same redox-active  $\text{Co}_6\text{Te}_8$  core, but the Co ions are capped with bulkier phosphines. Reaction of this larger donating superatom with the acceptor  $\text{Fe}_8\text{O}_4\text{pz}_{12}\text{Cl}_4$  gives large hexagonal black plates that are 1:1 combinations of  $\text{Co}_6\text{Te}_8(\text{P}^n\text{Pr}_3)_6$  and  $\text{Fe}_8\text{O}_4\text{pz}_{12}\text{Cl}_4$ , as measured by SCXRD (Figure 3b–e). In this crystal, the two clusters form alternating hexagonal close-packed layers with an unusual sequence of stacking along the *c*-axis. The cluster  $\text{Co}_6\text{Te}_8(\text{P}^n\text{Pr}_3)_6$  adopts an ABACA (hc) double-hexagonal close-packed arrangement, and the cluster  $\text{Fe}_8\text{O}_4\text{pz}_{12}\text{Cl}_4$  follows the sequence A'A'B'B'A'A'. The combined stacking sequence is thus AB'BB'AA'CA' (hccc). The lattice parameter within each hexagonal layer is 21.46 Å, and the shortest centroid-to-centroid distance between two neighboring complementary clusters is 12.86 Å. It is worth noting that this compound belongs to one of only 10 pyroelectric<sup>27</sup> (or polar) point groups,  $C_{3v}$  (or  $3m$ ).

To understand the formation of these binary compounds, we used a combination of CV, electronic absorption spectroscopy, and crystallography. Our CV data suggest that the cobalt chalcogenide clusters transfer one electron to  $\text{Fe}_8\text{O}_4\text{pz}_{12}\text{Cl}_4$  (see Figure 1). Here we present further characterization of the compound  $[\text{Co}_6\text{Te}_8(\text{PET}_3)_6][\text{Fe}_8\text{O}_4\text{pz}_{12}\text{Cl}_4]$  supporting this observation, and we note that analogous results were obtained for all our materials.

We verified that the binary hierarchical lattice of  $[\text{Co}_6\text{Te}_8(\text{PET}_3)_6][\text{Fe}_8\text{O}_4\text{pz}_{12}\text{Cl}_4]$  forms via a one-electron-transfer process by comparing its electronic absorption spectrum with those of model compounds  $[\text{CoCp}_2]-[\text{Fe}_8\text{O}_4\text{pz}_{12}\text{Cl}_4]$  and  $[\text{CoCp}_2]_2[\text{Fe}_8\text{O}_4\text{pz}_{12}\text{Cl}_4]$  (Figures S15, S18, and S19). The cluster  $\text{Fe}_8\text{O}_4\text{pz}_{12}\text{Cl}_4$  is composed of a cubic core of four high-spin  $\text{Fe}^{\text{III}}$  metal centers bridged by four  $\mu_4$ -oxo ligands. A one-electron reduction of  $\text{Fe}_8\text{O}_4\text{pz}_{12}\text{Cl}_4$  delocalizes the transferred electron between the metal ions in the redox-active  $\text{Fe}_4\text{O}_4$  core, giving rise to an intervalence charge-transfer (IVCT) band centered around 1650 nm.<sup>28</sup> Electronic absorption spectroscopy reveals that the IVCT band present in the near-infrared (NIR) region of the  $[\text{CoCp}_2]-[\text{Fe}_8\text{O}_4\text{pz}_{12}\text{Cl}_4]$  spectrum is absent in that of  $[\text{CoCp}_2]_2[\text{Fe}_8\text{O}_4\text{pz}_{12}\text{Cl}_4]$ . The electronic absorption spectra of  $[\text{Co}_6\text{Te}_8(\text{PET}_3)_6][\text{Fe}_8\text{O}_4\text{pz}_{12}\text{Cl}_4]$  dissolved in dichloromethane as well as dispersed in KBr similarly show a weak, broad IVCT band centered around 1650 nm. This IVCT transition, characteristic of a Robin and Day class II compound<sup>28</sup> between the oxo-bridged Fe ions, confirms the presence of the monoanion  $[\text{Fe}_8\text{O}_4\text{pz}_{12}\text{Cl}_4]^-$  in  $[\text{Co}_6\text{Te}_8(\text{PET}_3)_6][\text{Fe}_8\text{O}_4\text{pz}_{12}\text{Cl}_4]$ . The lengthening of the Co–P and Fe–Cl bonds in the crystal structure of  $[\text{Co}_6\text{Te}_8(\text{PET}_3)_6]-[\text{Fe}_8\text{O}_4\text{pz}_{12}\text{Cl}_4]$  compared to the neutral clusters provides further evidence<sup>28,29</sup> of the presence of these superatomic ions in the solid state.

Our binary solids are assembled from superatomic ions with multiple reversible redox states. The solubility of these crystals in dichloromethane allows us to measure their redox properties using CV. Figure 4 shows a typical cyclic voltammogram measured for  $[\text{Co}_6\text{Te}_8(\text{P}^n\text{Pr}_3)_6][\text{Fe}_8\text{O}_4\text{pz}_{12}\text{Cl}_4]$ . This compound exhibits eight reversible redox couples that correspond

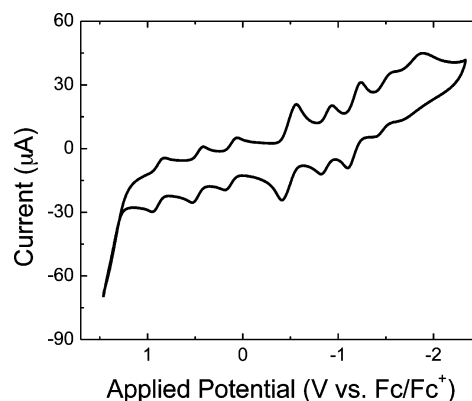


**Figure 4.** Cyclic voltammogram of  $[\text{Co}_6\text{Te}_8(\text{P}^n\text{Pr}_3)_6][\text{Fe}_8\text{O}_4\text{pz}_{12}\text{Cl}_4]$  (in 0.1 M  $t\text{Bu}_4\text{NPF}_6/\text{DCM}$ , scan rate 200 mV/s, glassy carbon working electrode, measured versus  $\text{Fc}/\text{Fc}^+$ ).

to the shuttling of nine electrons into and out of the cluster units. While these redox processes were measured in solution, we anticipate that similar behaviors exist in the crystals and could lead to the creation of cluster-assembled intercalation compounds.<sup>1</sup>

By combining molecular clusters with complementary electronic properties, we have synthesized binary solid-state compounds whose infinite crystalline structures are defined on both the superatomic and atomic scales. The packing of clusters with the same physical profile is robust to changes in the elements that populate the inorganic cores. By capitalizing on the synthetic variability of individual clusters, we have incorporated multiple redox-active clusters into a diverse family of solid-state materials. We have further shown that subtle variations of the capping ligands on cluster cores produce significant changes in the atomic structure and the superatomic packing, such as the adoption of a configuration that has symmetry-allowing pyroelectrical behavior. With a virtually limitless library of ligands available, the structures of these solid-state compounds become more versatile as one can imagine controlling cluster arrangements with great precision.

## ■ ASSOCIATED CONTENT

### 📄 Supporting Information

Synthetic details, characterization, and crystallographic (CIF) files. This material is available free of charge via the Internet at <http://pubs.acs.org>.

## ■ AUTHOR INFORMATION

### Corresponding Author

xr2114@columbia.edu

### Notes

The authors declare no competing financial interest.

## ■ ACKNOWLEDGMENTS

This material is based upon work supported by the Air Force Office of Scientific Research under AFOSR Award No. FA9550-14-1-0381. A.T. thanks the Société de Chimie Industrielle scholarship program and the Columbia University Egleston Scholars program. G.E. is supported by the Columbia Optics and Quantum Electronics IGERT program and the NRI/Hans J. Coufal Fellowship. T.B. and T.S. are supported by the U.S. Department of Energy, Office of Basic Sciences, under Contract No. DE-SC0008832, the State of Florida, and Florida



State University. D.W.P. thanks the Guthikonda family for funding and Dr. Joshua Palmer for many helpful discussions. X-ray diffraction studies were performed at the Advanced Materials Laboratory at FSU and the Shared Materials Characterization Laboratory at Columbia University. Use of the Shared Materials Characterization Laboratory was made possible by the funding from Columbia University.

## REFERENCES

- (1) Claridge, S. A.; Castleman, A. W.; Khanna, S. N.; Murray, C. B.; Sen, A.; Weiss, P. S. *ACS Nano* **2009**, *3*, 244.
- (2) Chevrel, R.; Sergent, M.; Hirrien, M. *J. Solid State Chem.* **1971**, *3*, 515.
- (3) Schäfer, H.; Eisenman, B.; Müller, W. *Angew. Chem. Int. Ed.* **1973**, *12*, 694.
- (4) Petrovic, A. P.; Lortz, R.; Santi, G.; Berthod, C.; Dubois, C.; Decroux, M.; Demuer, A.; Antunes, A. B.; Pare, A.; Salloum, D.; Gougeon, P.; Potel, M.; Fisher, O. *Phys. Rev. Lett.* **2011**, *106*, No. 017003.
- (5) Wang, J.; Liu, X. C.; Xia, S. Q.; Tao, X. T. *J. Am. Chem. Soc.* **2013**, *135*, 11840.
- (6) Talapin, D. V.; Lee, J. S.; Kovalenko, M. V.; Shevchenko, E. V. *Chem. Rev.* **2010**, *110*, 389.
- (7) Choi, C. L.; Alivisatos, A. P. *Annu. Rev. Phys. Chem.* **2010**, *61*, 369.
- (8) Auyeung, E.; Cutler, J. I.; Macfarlane, R. J.; Jones, M. R.; Wu, J.; Liu, G.; Zhang, K.; Osberg, K. D.; Mirkin, C. A. *Nat. Nanotechnol.* **2012**, *7*, 24.
- (9) Kang, Y. J.; Ye, X. C.; Chen, J.; Qi, L.; Diaz, R. E.; Doan-Nguyen, V.; Xing, G. Z.; Kagan, C. R.; Li, J.; Gorte, R. J.; Murray, C. B. *J. Am. Chem. Soc.* **2013**, *135*, 1499.
- (10) Degroot, M. W.; Corrigan, J. F. In *Comprehensive Coordination Chemistry II*; McCleverty, J. A., Meyer, T. J., Eds.; Pergamon: Oxford, 2003; Vol. 7, pp 57–123.
- (11) Reber, A. C.; Khanna, S. N.; Castleman, A. W. *J. Am. Chem. Soc.* **2007**, *129*, 10189.
- (12) Reveles, J. U.; Clayborne, P. A.; Reber, A. C.; Khanna, S. N.; Pradhan, K.; Sen, P.; Pederson, M. R. *Nat. Chem.* **2009**, *1*, 310.
- (13) Beaudron, S. A.; Batail, P.; Coulon, C.; Clerac, R.; Canadell, E.; Laukhin, V.; Melzi, R.; Wzietek, P.; Jerome, D.; Auban-Senzier, P.; Ravy, S. *J. Am. Chem. Soc.* **2005**, *127*, 11785.
- (14) Zheng, Z. P.; Long, J. R.; Holm, R. H. *J. Am. Chem. Soc.* **1997**, *119*, 2163.
- (15) Yoon, B.; Luedtke, W. D.; Barnett, R. N.; Gao, J.; Desireddy, A.; Conn, B. E.; Bigioni, T.; Landman, U. *Nat. Mater.* **2014**, *13*, 807.
- (16) Long, D. L.; Burkholder, E.; Cronin, L. *Chem. Soc. Rev.* **2007**, *36*, 105.
- (17) Jin, S.; DiSalvo, F. J. *Chem. Mater.* **2002**, *14*, 3448.
- (18) Schulz-Dobrick, M.; Jansen, M. *Eur. J. Inorg. Chem.* **2006**, 4498.
- (19) Schulz-Dobrick, M.; Jansen, M. *Inorg. Chem.* **2007**, *46*, 4380.
- (20) Wang, L.; Wu, T.; Bu, X. H.; Zhao, X.; Zuo, F.; Feng, P. Y. *Inorg. Chem.* **2013**, *52*, 2259.
- (21) Liu, H.; Hsu, C.-H.; Lin, Z.; Shan, W.; Wang, J.; Jiang, J.; Huang, M.; Lotz, B.; Yu, X.; Zhang, W.-B.; Yue, K.; Cheng, S. Z. D. *J. Am. Chem. Soc.* **2014**, *136*, 10691.
- (22) Roy, X.; Lee, C. H.; Crowther, A. C.; Schenck, C. L.; Besara, T.; Lalancette, R. A.; Siegrist, T.; Stephens, P. W.; Brus, L. E.; Kim, P.; Steigerwald, M. L.; Nuckolls, C. *Science* **2013**, *341*, 157.
- (23) Steigerwald, M. L.; Siegrist, T.; Stuczynski, S. M. *Inorg. Chem.* **1991**, *30*, 4940.
- (24) Roy, X.; Schenck, C. L.; Ahn, S.; Lalancette, R. A.; Venkataraman, L.; Nuckolls, C.; Steigerwald, M. L. *Angew. Chem. Int. Ed.* **2012**, *51*, 12473.
- (25) Baran, P.; Boca, R.; Chakraborty, I.; Giapintzakis, J.; Herchel, R.; Huang, Q.; McGrady, J. E.; Raptis, R. G.; Sanakis, Y.; Simopoulos, A. *Inorg. Chem.* **2008**, *47*, 645.
- (26) Wells, A. F. *Structural Inorganic Chemistry*, 5th ed.; Oxford Univ. Press: Oxford, 1984.
- (27) Whatmore, R. W. *Rep. Prog. Phys.* **1986**, *49*, 1335.
- (28) Chakraborty, I.; Baran, P.; Sanakis, Y.; Simopoulos, A.; Fachini, E.; Raptis, R. G. *Inorg. Chem.* **2008**, *47*, 11734.
- (29) Orpen, A. G.; Connelly, N. G. *Organometallics* **1990**, *9*, 1206.